

Resonance Raman characterization of five-coordinate dioxygen adducts of porphyrinatocobalt(II) complexes formed in low temperature O₂ matrices†

Leonard M. Proniewicz,^{a,*} Antoni Kulczycki,^c Aleksandra Weselucha-Birczyńska,^b Halina Majcherczyk^a and Kazuo Nakamoto^{*d}

^a Chemical Physics Division, Department of Chemistry, Jagiellonian University, 3 Ingardena Str., 30-060 Cracow, Poland

^b Regional Laboratory of Physicochemical Analysis and Structural Research, Jagiellonian University, 3 Ingardena Str., 30-060 Cracow, Poland

^c Institute of Material Science and Ceramics, University of Mining and Metallurgy (AGH), 30 Mickiewicz Ave., 30-059 Cracow, Poland

^d Chemistry Department, Marquette University, Milwaukee, WI 53201-1881, USA

Received (in Montpellier, France) 2nd July 1998, Accepted 29 September 1998

Resonance Raman (RR) spectra of five-coordinate dioxygen adducts of cobalt(tetramesitylporphine) and cobalt(tetramesopropylporphine) formed in low temperature O₂ matrices are reported. For the first time, all three vibrations expected for the Co—O₂ fragment, $\nu(\text{O—O})$, $\nu(\text{Co—O}_2)$ and $\delta(\text{Co—O—O})$, were observed for ¹⁶O₂ and ¹⁸O₂ isotopomers. These bands have been assigned based on oxygen isotope shift data as well as normal coordinate analysis of the Co—O₂ moiety. This work presents also the first observation of two distinct $\nu(\text{O—O})$ bands due to the Co—¹⁶O—¹⁸O and Co—¹⁸O—¹⁶O isomers in 'end-on' type dioxygen adducts. The mechanism of resonance enhancement, the effect of the axial ligand on the $\nu(\text{O—O})$ and $\nu(\text{Co—O}_2)$ frequencies and the differences in metal—O₂ bonding between cobalt and iron porphyrins are discussed.

Resonance Raman (RR) spectroscopy is a potentially effective probe for studying the structure and bonding of dioxygen adducts of heme proteins and their model compounds.¹ In favourable cases, spectral features associated with $\nu(\text{O—O})$, $\nu(\text{M—O}_2)$ and $\delta(\text{M—O—O})$ (M being a metal), where ν and δ are stretching and bending vibrations, respectively, can be identified in the RR spectra by using isotopically labeled compounds. Unfortunately, resonance enhancement of the $\nu(\text{O—O})$ mode of native heme proteins and iron porphyrins has not been successful for those containing nitrogeneous axial ligands. This is probably due to the absence of the Fe—O₂ charge transfer (CT) transition in the visible range.² However, the $\nu(\text{Fe—O}_2)$ and $\delta(\text{Fe—O—O})$ vibrations have been observed for a number of heme proteins.^{3,4} On the other hand, the $\nu(\text{O—O})$ and $\nu(\text{Co—O}_2)$ vibrations of dioxygen adducts of Co-substituted hemoglobin, myoglobin and their model compounds can be resonance enhanced.^{5–7} However, these spectra are rather difficult to interpret because of the appearance of several oxygen isotope sensitive bands that arise from vibrational coupling between $\nu(\text{O—O})$ and internal modes of the nitrogeneous axial ligand.^{8–10}

Although a large amount of RR data is available on six-coordinate dioxygen adducts of cobalt porphyrins, only two studies have been reported, thus far, on five-coordinate Co(porphyrin)O₂^{11,12} since these compounds are extremely unstable and can be formed only in low temperature matrices. The $\nu(\text{Co—O}_2)$ stretch of Co(TPP)O₂, where TPP denotes the tetraphenylporphinato dianion, was first assigned to the band at 345 cm⁻¹ in the RR spectrum of Co(TPP) cocondensed with O₂ in a low temperature O₂ matrix.¹¹ Recently, by using a β -pyrrole deuteriated analogue of TPP, TPP-d₈, which has no vibrations in the 350 cm⁻¹ region, we¹² were able to show that the 345 cm⁻¹ band is due to a TPP macro-

cycle mode. At that time we could not locate the $\nu(\text{Co—}^{16}\text{O}_2)$ vibration because it is very weak and overlapped by a strong TPP-d₈ band at 383 cm⁻¹. However, the broad shoulder at 369 cm⁻¹, observed for the ¹⁸O₂ adduct only, was assigned to the $\nu(\text{Co—}^{18}\text{O}_2)$ mode of Co(TPP-d₈)¹⁸O₂.¹²

In this work we report the simultaneous observation of all three modes expected for the Co—O₂ moiety, $\nu(\text{O—O})$, $\nu(\text{Co—O}_2)$ and $\delta(\text{Co—O—O})$, of five-coordinate Co(TMP)O₂ and Co(MPR)O₂, where TMP and MPR denote the tetramesitylporphinato and tetramesopropylporphinato dianions, respectively. Our assignments are based on ¹⁶O₂/¹⁸O₂ isotope shifts. We also performed normal coordinate analysis (NCA) based on the generalized valence force field (GVFF) model¹³ and discuss the effect of the Co—O—O bond angle variation on the Co—O₂ stretching frequency. Additionally, we calculated potential energy distributions (PED) by using a standard procedure¹⁴ to estimate the degree of vibrational mixing between $\nu(\text{Co—O}_2)$ and $\delta(\text{Co—O—O})$.

Experimental

Compounds

H₂TMP was synthesized by the method of Hill and Williamson.¹⁵ To remove tetramesitylchlorine contamination, H₂TMP was refluxed with 2,3-dichloro-5,6-dicyano-1,4-benzoquinone (DDQ) in toluene, extracted with sodium dithionite and then chromatographed over basic alumina with freshly distilled dichloromethane.¹⁶ H₂MPR was purchased from Midcentury (Posen, IL) and used without further purification.

The cobalt complexes of these porphyrins were prepared by reaction of cobalt(II) chloride, CoCl₂, with the respective porphyrin in the presence of 2,6-dimethylpyridine in refluxing dry tetrahydrofuran, THF, under a nitrogen atmosphere. The complexes obtained were then purified by chromatography on

† Non-SI unit employed: 1 Torr \approx 133 Pa.

an alumina column according to the procedure of Collman *et al.*¹⁷

Samples of $^{16}\text{O}_2$ (prepurified, 99.9%) and $^{18}\text{O}_2$ (97% pure) were purchased from Matheson Gas and ICON Services, respectively. 'Scrambled' dioxygen ($^{16}\text{O}_2 : ^{16}\text{O}^{18}\text{O} : ^{18}\text{O}_2 = 1 : 2 : 1$) was prepared *via* electrical discharge of an equimolar mixture of $^{16}\text{O}_2$ and $^{18}\text{O}_2$. Ozone formed during this process was decomposed by activated 4A molecular sieves inserted into a reaction flask. The final mixing ratio of all oxygen isotopic molecules was determined by Raman measurements of the reaction mixture.

Spectral measurements

RR spectra of five-coordinate base-free dioxygen adducts of cobalt porphyrins were obtained by using the miniature oven technique.¹⁸ Thus, a sample of porphyrinatocobalt(II) was placed in a miniature graphite oven and heated to about 150–180 °C in a vacuum ($\approx 10^{-5}$ Torr) to remove any volatile contaminants. Then, the sample was vaporized by heating the oven to 300–350 °C and co-condensed with O_2 on a copper cold tip, which was cooled to about 25 K by a CTI Model 21 closed-cycle helium refrigerator. A back-scattering geometry was set up with a cylindrical lens to produce a line focus on the sample surface to avoid possible thermal decomposition of the samples.¹⁹

RR spectra were recorded on a Spex Model 1403 double monochromator fitted with a Hamamatsu R-928 photomultiplier and a Spex DM1B computer. Four scans were accumulated to obtain the RR spectra presented in this work. A Coherent Innova 100-K3 krypton ion laser was used for 406.7 nm excitation. The power at the sample was kept at *ca.* 5 mW. A spectral band pass of 4 cm^{-1} was routinely used. The accuracy of a frequency reading was $\pm 1 \text{ cm}^{-1}$.

Results and discussion

Co(TMP) O_2

The RR spectrum (406.7 nm excitation) of the $^{16}\text{O}_2$ adduct of Co(TMP) is shown in Fig. 1(A). In the high frequency region this adduct is characterized by the band at 1270 cm^{-1} , which is shifted to 1200 cm^{-1} upon $^{16}\text{O}_2/^{18}\text{O}_2$ substitution [Fig. 1(B)]. These bands are easily identified as $\nu(^{16}\text{O}-^{16}\text{O})$ and $\nu(^{18}\text{O}-^{18}\text{O})$, respectively, of Co(TMP) O_2 . The observed isotopic shift of 70 cm^{-1} is in good agreement with the theoretically predicted value for the O—O diatomic harmonic oscillator (72 cm^{-1}). These frequencies are also in good agreement with those reported previously for Co(TPP- d_8) O_2 (RR studies¹²), Co(TPP) O_2 and Co(OEP) O_2 (IR studies^{11,20}).

As was demonstrated previously,¹¹ the dioxygen in 'base-free' Co(TPP) O_2 takes an end-on geometry. This is based on the evidence that when a metal porphyrin reacts with $^{16}\text{O}^{18}\text{O}$ in scrambled dioxygen, the end-on adduct having non-equivalent oxygen atoms exhibits two $\nu(^{16}\text{O}-^{18}\text{O})$ bands [namely $\nu(\text{metal})-^{16}\text{O}-^{18}\text{O}$] and $\nu(\text{metal})-^{18}\text{O}-^{16}\text{O}$], while the side-on adduct, having equivalent oxygen atoms, shows only one $\nu(^{16}\text{O}-^{18}\text{O})$. In this study we also performed experiments with scrambled dioxygen [Fig. 1(C)]. In the high frequency region, two new bands appear in addition to those already discussed. One is clearly observed at 1241 cm^{-1} , while the second occurs at around 1230 cm^{-1} as a shoulder on the 1234 cm^{-1} porphyrin band. Thus, these bands are readily assignable to the $\nu[(\text{Co})-^{16}\text{O}-^{18}\text{O}]$ and $\nu[(\text{Co})-^{18}\text{O}-^{16}\text{O}]$ vibrations, respectively.^{11,21} The present results clearly demonstrate that the O_2 molecule binds to Co(TMP) in the asymmetric end-on fashion. Such end-on structures are also known for six-coordinate dioxygen adducts of cobalt porphyrins,^{1,8–10} cobalt-substituted heme proteins^{1,5–7} and cobalt Schiff bases of the η^1 type.^{22–25} However, this is the first report on the RR observation of two

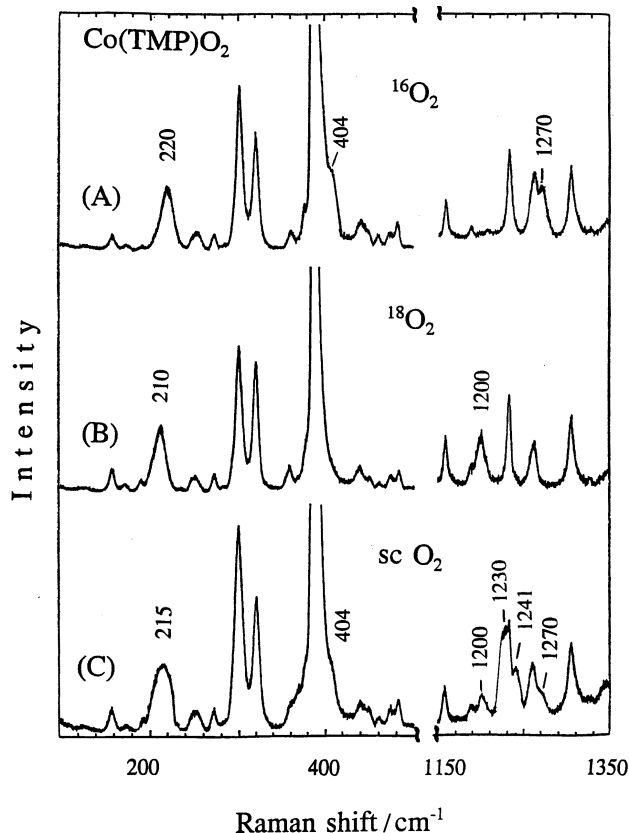


Fig. 1 Resonance Raman spectra of Co(TMP) co-condensed with dioxygen at 25 K (406.7 nm excitation). (A) $^{16}\text{O}_2$; (B) $^{18}\text{O}_2$; (C) scrambled O_2 .

non-equivalent $\nu(^{16}\text{O}-^{18}\text{O})$, which are characteristic of the end-on dioxygen geometry.

In the low frequency region the RR spectrum of the $^{16}\text{O}_2$ adduct of Co(TMP) exhibits two oxygen isotope sensitive bands at 404 (as a shoulder on a very strong porphyrin band at around 390 cm^{-1}) and 220 cm^{-1} [Fig. 1(A)]. Upon $^{16}\text{O}_2/^{18}\text{O}_2$ substitution these bands are downshifted; the 404 cm^{-1} band disappears since it is apparently shifted under the strong 390 cm^{-1} macrocycle band, while the 220 cm^{-1} band is shifted to 210 cm^{-1} . Based on our previous work¹² and also on NCA calculations (*vide infra*), we assign the 404 and 220 cm^{-1} bands to the $\nu(\text{Co}-^{16}\text{O}_2)$ and $\delta(\text{Co}-^{16}\text{O}-^{16}\text{O})$ modes, respectively. We also tried to determine the $\nu(\text{Co}-^{18}\text{O}_2)$ frequency from the difference spectrum (A) – (B) and by using a fitting procedure. However, due to inadequate experimental conditions we were not able to get a clear-cut result.

When scrambled oxygen is used [Fig. 1(C)] the band at 404 cm^{-1} practically disappears since its intensity is 1/4 of that presented in Fig. 1(A). Obviously, the expected $\nu(\text{Co}-^{16}\text{O}^{18}\text{O})$ and $\nu(\text{Co}-^{18}\text{O}^{16}\text{O})$ bands are hidden under the porphyrin band. Thus, the only oxygen isotope sensitive band seen is at 215 cm^{-1} . Although four Co—O—O bending vibrations are expected when scrambled dioxygen is reacted with the cobalt(II) porphyrin, we observe only a broad and symmetric band at 215 cm^{-1} since their frequencies are expected to be close (within 10 cm^{-1}).

Co(MPR) O_2

Next we measured the RR spectra of Co(MPR) O_2 to observe the $\nu(\text{Co}-^{16}\text{O}_2)$ and $\nu(\text{Co}-^{18}\text{O}_2)$ vibrations, which are expected to have less interference from the porphyrin core deformation mode near 390 cm^{-1} .^{1,26} Fig. 2(A) shows the RR spectrum (406.7 nm excitation) of the $^{16}\text{O}_2$ adduct of Co(MPR). It exhibits three bands at 1262, 402 (shoulder) and

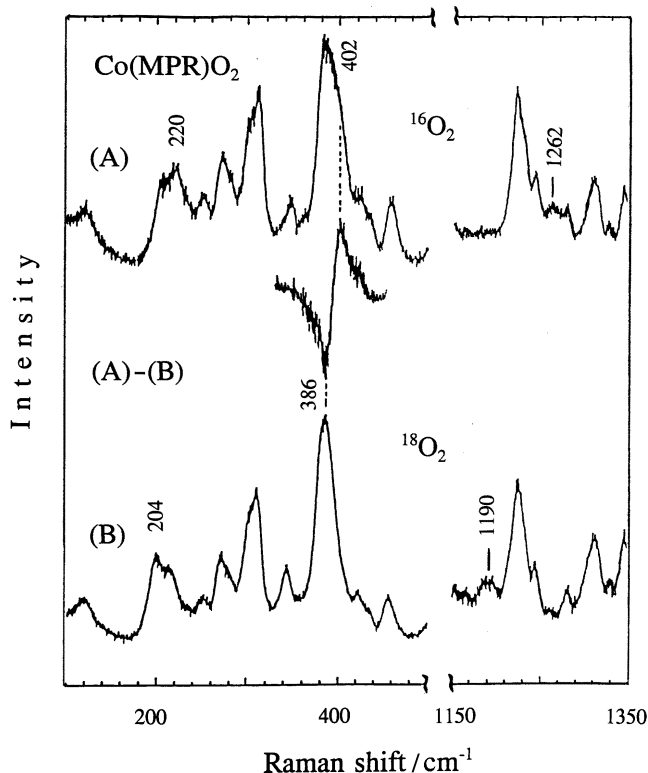


Fig. 2 Resonance Raman spectra of Co(MPR) co-condensed with dioxygen at 25 K (406.7 nm excitation). (A) $^{16}\text{O}_2$; (B) $^{18}\text{O}_2$. (A) – (B) is the difference spectrum.

220 cm^{-1} . These bands are identified as the $\nu(^{16}\text{O}-^{16}\text{O})$, $\nu(\text{Co}-^{16}\text{O}_2)$ and $\delta(\text{Co}-^{16}\text{O}-^{16}\text{O})$ modes, respectively, confirming our previous assignments.¹² Upon $^{16}\text{O}_2/^{18}\text{O}_2$ substitution these bands are shifted to 1190, 386 and 204 cm^{-1} , respectively [Fig. 2(B)]. As can be seen in the middle trace, the difference spectrum (A) – (B) clearly shows the presence of two bands at 402 and 386 cm^{-1} .

Mechanism of RR enhancement

Fig. 1 and 2 show that only weak RR enhancement can be achieved for all three modes expected for the $\text{Co}-\text{O}_2$ moiety of $\text{Co}(\text{TMP})\text{O}_2$ and $\text{Co}(\text{MPR})\text{O}_2$ by using 406.7 nm excitation. No marked differences were noted for RR enhancements by excitation at 413.1 and 415.4 nm .

Thus far, at least three mechanisms have been proposed to account for resonance enhancement of axial vibrations such as $\nu(\text{Co}-\text{O}_2)$ in metalloporphyrin complexes, namely one direct and two indirect mechanisms. The direct mechanism assumes the presence of a metal– O_2 charge transfer (CT) transition. In cobalt porphyrins, the axial ligand (L) \rightarrow Co CT transition may occur from filled σ or π ligand orbitals to vacant metal d orbitals, whereas $\text{Co} \rightarrow$ L CT transition may occur from the partially filled d orbitals to vacant π ligand orbitals.¹ Since such CT transitions are localized in the $\text{Co}-\text{L}$ linkage, the $\text{Co}-\text{L}$ distance is expected to change appreciably when the laser wavelength is chosen in the $\text{Co} \rightarrow$ L CT region.²⁷ Although we have not been able to measure the electronic spectrum of $\text{Co}(\text{porphyrin})\text{O}_2$ in low temperature O_2 matrices, we anticipate the presence of a strong Soret band at around 410 nm for arylporphyrins and around 390 nm for alkylporphyrins.²⁸ The fact that the $\nu(\text{Co}-\text{O}_2)$ and $\nu(\text{O}-\text{O})$ vibrations are only weakly enhanced by violet lines from a krypton ion laser does not necessarily exclude the direct mechanism of RR enhancement of these modes. However, a very weak enhancement of these vibrations in $\text{Co}(\text{MPR})\text{O}_2$ by violet lines (practically no enhancement by using argon ion blue and green lines) and the observation of $\nu(\text{O}-\text{O})$ upon yellow exci-

tation (*vide infra*) seem to suggest that the direct mechanism is not responsible for the observed phenomenon. It is interesting to note that the $\nu(\text{Co}-\text{O}_2)$ and $\nu(\text{O}-\text{O})$ stretches of (six-coordinate) oxycobaltmyoglobin, CoMbO_2 , and oxycobalthemoglobin, CoHbO_2 , are enhanced through the $\text{L} \rightarrow \text{Co}$ CT transition [$\pi^*(\pi_g^*\text{O}_2/d_{xz}) \rightarrow \sigma^*(d_{z^2}\text{Co}/\pi_g^*)$] underlying the Soret band.⁵ These observations seem to suggest that the nature of the $\text{Co}-\text{O}_2$ CT transition is affected strongly upon coordination of a base ligand in the position *trans* to the bound dioxygen.

In metal(porphyrin) L_2 (D_{4h} symmetry) or metal(porphyrin)L (C_{4v} symmetry) complexes, the out-of-plane vibration (A_{1g} and A_{1v} , respectively) can couple with in-plane porphyrin core vibrations of the same symmetry and borrow intensity from the latter.²⁹ Spiro³⁰ suggests, however, that such vibrational coupling would be rather weak since the internal coordinates are orthogonal. He prefers direct coupling of the axial ligand vibration to the in-plane electronic transition. Thus, in $\text{Co}(\text{porphyrin})\text{O}_2$, the $\nu(\text{Co}-\text{O}_2)$ mode of A_1 symmetry may be enhanced by the $\pi \rightarrow \pi^*$ transition of the porphyrin core since it alters the $\text{Co}-\text{O}$ and $\text{O}-\text{O}$ bond lengths. If so, their excitation profiles should follow that of the electronic absorption spectrum. Then the observed enhancement should be the strongest in the Soret region and become much weaker in the α and β regions.^{1,29} Even in the Soret region, however, excitation of the $\nu(\text{Co}-\text{O}_2)$ and $\nu(\text{O}-\text{O})$ modes is expected to be rather weak since the $\pi \rightarrow \pi^*$ transitions are highly localized in the porphyrin core. Thus, the $\text{Co}-\text{O}$ and $\text{O}-\text{O}$ bond distances may not change appreciably²⁷ and the RR enhancement of the $\nu(\text{Co}-\text{O}_2)$ and $\nu(\text{O}-\text{O})$ modes may be weak. In fact, we observed only a very weak $\nu(^{18}\text{O}-^{18}\text{O})$ band at 1200 cm^{-1} for $\text{Co}(\text{TMP})^{18}\text{O}_2$ with excitation at 568.2 nm from a krypton ion laser. This band disappears upon $^{18}\text{O}_2/^{16}\text{O}_2$ isotopic substitution. Obviously, the $\nu(^{16}\text{O}-^{16}\text{O})$ band is too weak to be observed, since it is hidden under a medium to strong porphyrin band (probably B_{2g} mode, which corresponds to ν_{27} of the TPP macrocycle).³¹ Thus, we conclude that the $\nu(\text{Co}-\text{O}_2)$ and $\nu(\text{O}-\text{O})$ modes of five-coordinate dioxygen adducts of $\text{Co}(\text{porphyrins})$ are probably resonance enhanced through the indirect mechanism proposed by Spiro.³⁰

Influence of ligand basicity on the $\nu(\text{O}-\text{O})$ frequency

When the O_2 molecule binds to $\text{Co}(\text{II}) (d^7)$, the $\text{Co}-\text{O}_2$ bond is formed mainly by σ donation from $d_{z^2}(\text{Co})$ to the antibonding $\pi_g^*(\text{O}_2)$ orbital, which is only slightly counteracted by π donation in the opposite direction. There is abundant evidence to indicate that nearly one electron is transferred to the dioxygen *via* σ -bonding.^{22,23} Thus, the canonical form of the dioxygen adduct can be expressed as $\text{Co}(\text{III})-\text{O}_2^-$. In general, the $\nu(\text{O}-\text{O})$ frequency decreases as the negative charge on the $2p\pi^*$ orbital of dioxygen increases *via* electron donation from the porphyrin core through the Co atom. Thus, the more acidic the porphyrinato ligand, the less electron density on the metal ion and less σ donation to the dioxygen, resulting in a weaker $\text{Co}-\text{O}_2$ bond and a stronger $\text{O}-\text{O}$ bond. Accordingly, the observed order of the $\nu(\text{O}-\text{O})$ frequencies: $\text{Co}(\text{TPP-d}_8)\text{O}_2$ (1281 cm^{-1}) $>$ $\text{Co}(\text{OEP})\text{O}_2$ (1275 cm^{-1}) $>$ $\text{Co}(\text{TMP})\text{O}_2$ (1270 cm^{-1}) $>$ $\text{Co}(\text{MPR})\text{O}_2$ (1262 cm^{-1}) reflects the order of ligand basicity of these porphyrins. Although the opposite trend is expected for $\nu(\text{Co}-\text{O}_2)$,³² it was not possible to confirm it for five-coordinate $\text{Co}(\text{por})\text{O}_2$ since their frequencies were too close ($404 \pm 2-3\text{ cm}^{-1}$) (Table 1).

Normal coordinate analysis

Previously we carried out NCA on a triatomic $\text{Co}-\text{O}-\text{O}$ moiety of $\text{Co}(\text{MPR})\text{O}_2$ by using a set of four force constants.¹² In this work we performed NCA on a bent $\text{Co}-\text{O}-\text{O}$ fragment of $\text{Co}(\text{TMP})\text{O}_2$. Since no X-ray data are

Table 1 The $\nu(\text{O}-\text{O})$, $\nu(\text{M}-\text{O}_2)$, and $\delta(\text{M}-\text{O}-\text{O})$ frequencies (in cm^{-1}) of five-coordinate dioxygen adducts of cobalt and iron porphyrins

Compound	$\nu(\text{O}-\text{O})$	$\nu(\text{M}-\text{O}_2)$	$\delta(\text{M}-\text{O}-\text{O})$	References
$\text{Co}(\text{TPP-d}_8)\text{O}_2$	1281	?	216	12
$\text{Co}(\text{OEP})\text{O}_2$	1275	407	217	21, 12b
$\text{Co}(\text{TMP})\text{O}_2$	1270	404	220	this work
$\text{Co}(\text{MPR})\text{O}_2$	1262	402	220	this work
$\text{Fe}(\text{TPP-d}_8)\text{O}_2$	1195	508	345	19
$\text{Fe}(\text{OEP})\text{O}_2$	1192	509	?	19
$\text{Fe}(\text{TMP})\text{O}_2$	1188	516	343	19

available on five-coordinate $\text{Co}(\text{porphyrin})\text{O}_2$ complexes, we used the molecular parameters, which were varied in the following ranges: the $\text{O}-\text{O}$ distance (R_1) from 1.15 to 1.30 Å, the $\text{Co}-\text{O}$ distance (R_2) from 1.90 to 2.10 Å, and the $\text{Co}-\text{O}-\text{O}$ angle (θ) from 90° to 180° . Since we were not able to observe the $\nu(\text{Co}-^{18}\text{O}_2)$, these parameters were adjusted so that the calculated frequency of $\nu(\text{Co}-^{18}\text{O}_2)$ becomes 385 cm^{-1} , that is, almost the same frequency as that observed for $\text{Co}(\text{MPR})^{18}\text{O}_2$. The best fit of data including both dioxygen isotopomers was obtained for: $R_1 = 1.20 \text{ Å}$, $R_2 = 2.00 \text{ Å}$ and $\theta = 137.5^\circ$. These values are very close to those used in the $\text{Fe}(\text{Pc})\text{O}_2$ calculations,³³ where Pc is the phthalocyanato dianion. A set of six force constants obtained was: $K(R_1) = 7.43$, $K(R_2) = 1.63$, $H(\theta) = 0.26$, $K(R_1, R_2) = 0.10$, $K(R_1, \theta) = 1.8 \times 10^{-5}$, and $K(R_2, \theta) = 0.13 \text{ m dyn Å}^{-1}$. Then we calculated frequency dependences of the $\nu(^{16}\text{O}-^{16}\text{O})$, $\nu(\text{Co}-^{16}\text{O}_2)$, $\delta(\text{Co}-^{16}\text{O}-^{16}\text{O})$ modes (and the same for the $^{18}\text{O}_2$ derivative) as a function of θ . The results shown in Fig. 3 clearly indicate that the $\nu(\text{O}-\text{O})$ frequencies do not change much with variation of θ , whereas the $\nu(\text{Co}-\text{O}_2)$ and $\delta(\text{Co}-\text{O}-\text{O})$ frequencies change dramatically. For example, in the range from 130° to 150° , a slight change of θ (i.e., of 5°) induces a downshift of $\nu(\text{Co}-\text{O}_2)$ and an upshift of $\delta(\text{Co}-\text{O}-\text{O})$ by as much as 10 cm^{-1} . Thus, observation of these low frequency modes is highly important in estimating the $\text{Co}-\text{O}-\text{O}$ angle.

We also calculated the potential energy distributions (PED) for $\nu(^{16}\text{O}-^{16}\text{O})$, $\nu(\text{Co}-^{16}\text{O}_2)$ and $\delta(\text{Co}-^{16}\text{O}-^{16}\text{O})$ as a function of θ as presented in Fig. 4. These results show very small degrees of mixing among these three modes.

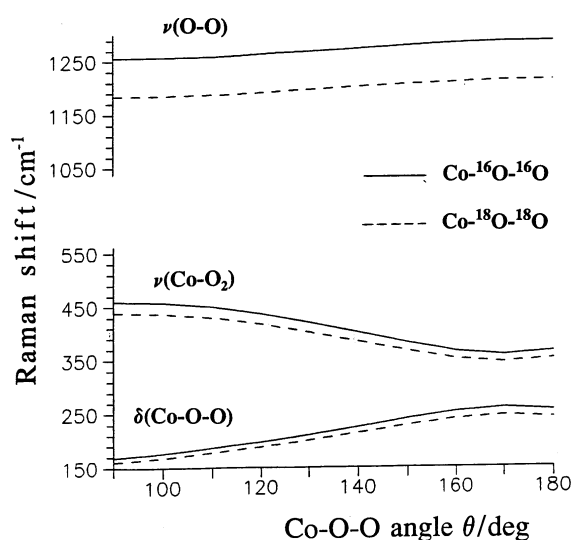


Fig. 3 Plots of theoretical $\nu(\text{O}-\text{O})$, $\nu(\text{Co}-\text{O}_2)$ and $\delta(\text{Co}-\text{O}-\text{O})$ as a function of the $\text{Co}-\text{O}-\text{O}$ angle (θ). The curves are calculated by using $K(\text{O}-\text{O})$, $K(\text{Co}-\text{O})$ and $H(\text{Co}-\text{O}-\text{O})$ values of 7.43, 1.63, and $0.26 \text{ m dyn Å}^{-1}$, respectively (see text for details).

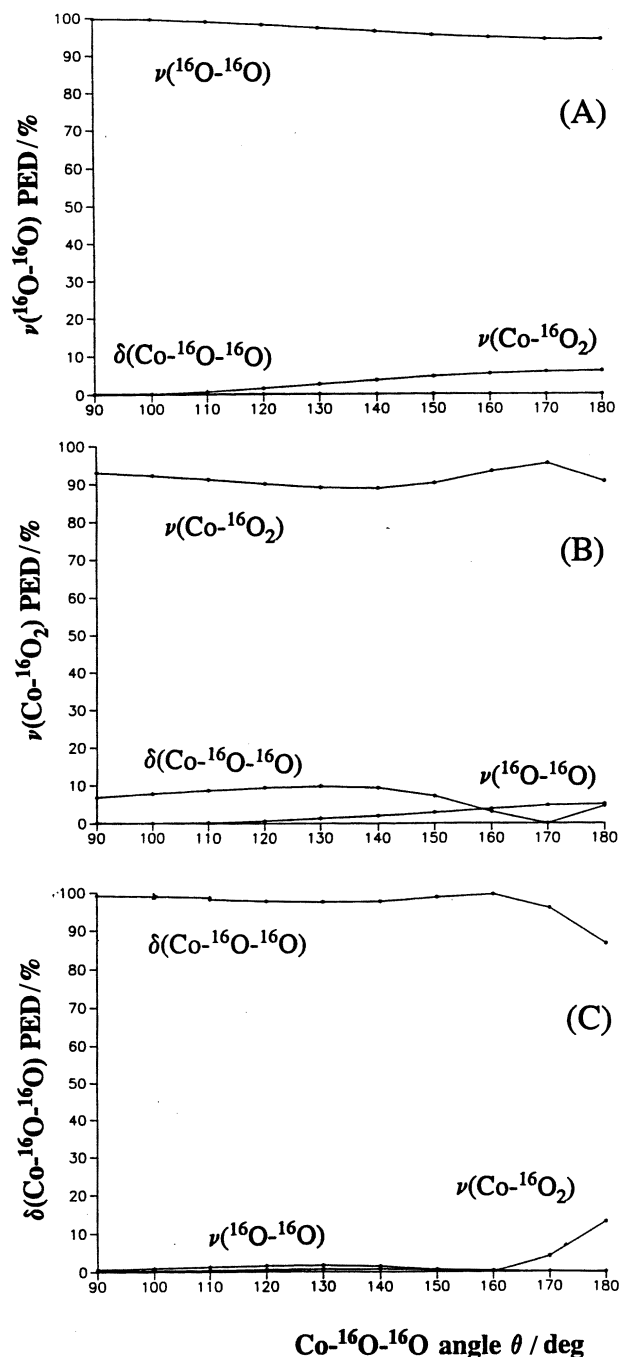


Fig. 4 Potential energy distributions (PED) for: (A) $\nu(^{16}\text{O}-^{16}\text{O})$; (B) $\nu(\text{Co}-^{16}\text{O}_2)$; (C) $\delta(\text{Co}-^{16}\text{O}-^{16}\text{O})$ as a function of the $\text{Co}-^{16}\text{O}-^{16}\text{O}$ angle (θ).

Metal ion effect: $\text{Co}(\text{III})$ versus $\text{Fe}(\text{III})$ in five- and six-coordinate porphyrin dioxygen adducts as heme protein model compounds

Five-coordinate $\text{M}(\text{porphyrin})\text{O}_2$ cannot be directly used as model compounds for heme proteins. However, they can serve as a potential probe for understanding the influence of the steric, electronic and other environmental factors on dioxygen binding in naturally occurring heme proteins. The main difficulty in studying these base-free compounds is that they are very unstable and can be obtained exclusively in low temperature matrices.

In contrast to $\text{Co}(\text{porphyrin})$, reaction of O_2 with $\text{Fe}(\text{porphyrin})$ in the gas phase leads to formation of two types of five-coordinate dioxygen adducts.^{19,21} The major product exhibits the $\nu(^{16}\text{O}-^{16}\text{O})$ mode in the $1188\text{--}1223 \text{ cm}^{-1}$ range, while the minor one shows it at around 1105 cm^{-1} .^{19,21} These

bands have been assigned to the end-on and the side-on isomers, respectively.²¹ The latter is thermally unstable and converts reversibly to the end-on isomer upon raising the temperature. These two Fe(porphyrin)O₂ isomers are formed because there are two possible electronic ground state configurations that have been proposed for the square planar Fe(TPP): (d_{xy})²(d_{xz}d_{yz})³(d_{z²})¹³⁴ and (d_{xy})²(d_{z²})²(d_{xy}d_{yz})².³⁵ The former tends to favour the formation of the end-on, whereas the latter tends to prefer the symmetric side-on structure. Since the energy gap between these two electronic states is small, both isomers are produced in the reaction of Fe(II)(porphyrin) with O₂. The nature of the Fe—O₂ bond in these end-on dioxygen adducts is not fully understood. However, it has been suggested^{22,23} that the Fe—O₂ bond is formed by σ donation from the antibonding π_g^* of O₂ to the 3d_{z²} orbital of the iron atom, which is counteracted by π donation from the iron 3d _{π} orbitals to the dioxygen antibonding π_g^* orbitals.

Table 1 lists the $\nu(\text{O—O})$, $\nu(\text{M—O}_2)$ and $\delta(\text{M—O—O})$ frequencies of the known Co and Fe(por)O₂ end-on adducts. As is clearly seen, all cobalt complexes exhibit $\nu(\text{O—O})$ at much higher and $\nu(\text{M—O}_2)$ at much lower frequencies than the corresponding iron complexes. In general, the $\nu(\text{O—O})$ frequency reflects the charge density on the dioxygen: the larger the negative charge on the 2p π_g^* orbital of dioxygen the lower the $\nu(\text{O—O})$ and the higher the $\nu(\text{M—O}_2)$ frequencies. Thus, the low $\nu(\text{M—O}_2)$ and high $\nu(\text{O—O})$ frequencies reflect weaker M—O₂ and stronger $\nu(\text{O—O})$ bonds in the Co than in the Fe complexes. In other words, the results presented in Table 1 suggest that the net negative charge on the dioxygen is less in the five-coordinate cobalt than in the analogous iron complexes.

When a base ligand (in most cases imidazole, pyridine or their derivatives) coordinates to the axial position (*trans* to dioxygen), the $\nu(\text{O—O})$ band shifts markedly to lower frequency while the $\nu(\text{M—O}_2)$ band shifts upward as shown in Table 2. These trends indicate clearly that the *trans* axial ligand increases electron donation to the metal d orbitals, thus enhancing the M—O₂ bond strength and consequently weakening the O—O bond by increasing the net negative charge on the antibonding π_g^* (O₂) orbitals. This effect was quantitatively demonstrated for a series of Co(TPP-d₈)(base)O₂ complexes, where the $\nu(\text{O—O})$ frequency decreased linearly as the pK_a of the base increased.⁴⁴

Observed changes in the $\nu(\text{O—O})$ and $\nu(\text{M—O}_2)$ frequencies are more dramatic for cobalt than iron complexes, as expected from the differences in the nature of the Co—O₂ and Fe—O₂ bonds.^{22,23} This metal ion effect must be attributed to the multiple bond character of the Fe—O₂ bond relative to the single Co—O₂ bond. In fact, the $\nu(\text{Fe—O}_2)$ mode is at around 570 cm⁻¹ while the $\nu(\text{Co—O}_2)$ mode is near 520 cm⁻¹

in M(por)(base)(O₂). Consequently, coordination of a base ligand causes a downshift of the $\nu(\text{O—O})$ band by 'only' 50 cm⁻¹ in iron complexes but by 100–150 cm⁻¹ in six-coordinate cobalt dioxygen compounds.

The metal—O₂ stretching frequencies of six-coordinate dioxygen adducts of cobaltous and ferrous porphyrin model compounds are in fairly good agreement with those of hemoglobin (HbO₂), myoglobin (MbO₂) and their cobalt analogues (Table 2). On the other hand, previous infrared⁴⁵ and RR studies^{5,7,19,46} of these compounds show several oxygen isotope sensitive bands in the $\nu(\text{O—O})$ region that have caused controversy in their assignments. Yu and coworkers^{5,6} and Potter *et al.*⁴⁵ attributed the observed multiple band pattern to two discrete conformers of the dioxygen adducts. Later, Kincaid and coworkers^{8–10} have shown that the observed spectra can be interpreted in terms of a single conformer and that the appearance of the multiple oxygen isotope sensitive bands arises from 'vibrational resonance coupling' of the $\nu(\text{O—O})$ mode with internal modes of the *trans*-axial histidylimidazole fragment. Using this approach the exact $\nu(\text{O—O})$ frequency can be calculated from the observed RR spectra. The existence of a single dioxygen conformer has also been confirmed by Miller and Chance⁴⁷ in their recent FT-IR studies on MbO₂.

Acknowledgements

This work was supported by grants 2P 303 060 05 from the Polish State Committee for Scientific Research (KBN) (to LMP) and DMB-8613743 from the National Science Foundation (to KN).

References

- See for example: (a) *Biological Applications of Raman Spectroscopy*, ed. T. G. Spiro, Wiley-Interscience, New York, 1987, vol. 3; (b) T. Kitagawa and T. Ogura, *Prog. Inorg. Chem.*, 1997, **45**, 431.
- D. A. Case, B. H. Huynh and M. Karplus, *J. Am. Chem. Soc.*, 1979, **101**, 4433.
- W. A. Oertling, R. T. Kean, R. Wever and G. T. Babcock, *Inorg. Chem.*, 1990, **29**, 2633.
- (a) S. Hirota, T. Ogura, E. H. Appelman, K. Shinzawa-Itoh, S. Yoshikawa and T. Kitagawa, *J. Am. Chem. Soc.*, 1994, **116**, 10564; (b) S. Jeyarajah, L. M. Proniewicz, H. Bronder and J. R. Kincaid, *J. Biol. Chem.*, 1994, **269**, 31047.
- M. Tsubaki and N.-T. Yu, *Proc. Natl. Acad. Sci. USA*, 1981, **78**, 3581.
- H. C. Mackin, M. Tsubaki and N.-T. Yu, *Biophys. J.*, 1983, **41**, 349.
- A. Bruha and J. R. Kincaid, *J. Am. Chem. Soc.*, 1988, **110**, 6006.
- L. M. Proniewicz, K. Nakamoto and J. R. Kincaid, *J. Am. Chem. Soc.*, 1988, **110**, 4541.
- L. M. Proniewicz, A. Bruha, K. Nakamoto, E. Kyuno and J. R. Kincaid, *J. Am. Chem. Soc.*, 1989, **111**, 7050.
- L. M. Proniewicz and J. R. Kincaid, *J. Am. Chem. Soc.*, 1990, **112**, 675.
- M. Kozuka and K. Nakamoto, *J. Am. Chem. Soc.*, 1981, **103**, 2162.
- (a) A. Weselucha-Birczyńska, K. Nakamoto and L. M. Proniewicz, *J. Mol. Struct.*, 1992, **275**, 95; (b) L. M. Proniewicz, A. Weselucha-Birczyńska, K. Nakamoto, in *XIIIth International Conference on Raman Spectroscopy*, eds N.-T. Yu and X.-Y. Li, J. Wiley and Sons, New York, 1992, p. 540.
- (a) A. Kulczycki, *Spectrochim. Acta, Part A*, 1985, **41**, 1427; (b) A. Kulczycki, *J. Mol. Struct.*, 1991, **263**, 151.
- Y. Morino and K. Kuchitsu, *J. Chem. Phys.*, 1952, **20**, 1809.
- C. L. Hill and M. M. Williamson, *J. Chem. Soc., Chem., Commun.*, 1985, 1228.
- K. Rousseau and D. Dolphin, *Tetrahedron Lett.*, 1974, **48**, 4251.
- J. P. Collman, J. I. Brauman, K. M. Doxsee, T. R. Halbert, S. E. Hayes and K. S. Suslick, *J. Am. Chem. Soc.*, 1978, **100**, 2761.
- W. Scheuermann and K. Nakamoto, *Appl. Spectrosc.*, 1978, **32**, 251.

Table 2 The $\nu(\text{O—O})$ and $\nu(\text{M—O}_2)$ frequencies (in cm⁻¹) of six-coordinate dioxygen adducts of various cobalt and iron porphyrins and heme proteins

Compound	$\nu(\text{O—O})$	$\nu(\text{M—O}_2)$	References
Co(OEP-d ₄)(py)O ₂	1145	521	36
Co(TPP)(pip)O ₂	1142	519	37
Co(PF)(DMI)O ₂	1151	527	36, 6
Fe(OEP)(pip)O ₂	?	574	38
Fe(TPP)(pip)O ₂	1157	575	37
Fe(PF)(NMI)O ₂	1159	568	39, 26
CoHbO ₂	1138	537	7, 19, 5
CoMbO ₂	1138	539	7, 5
HbO ₂	1107	567	40, 41
MbO ₂	1103	572	42, 43

Abbreviations: py = pyridine; pip = piperidine; DMI = 1,2-dimethylimidazole; NMI = N-methylimidazole; PF = 'picket-fence' porphyrin.

- 19 L. M. Proniewicz, I. R. Paeng and K. Nakamoto, *J. Am. Chem. Soc.*, 1991, **113**, 3294.
- 20 M. W. Urban, K. Nakamoto and J. R. Kincaid, *Inorg. Chim. Acta*, 1984, **61**, 77.
- 21 T. Watanabe, T. Ama and K. Nakamoto, *J. Phys. Chem.*, 1984, **88**, 440.
- 22 R. D. Jones, D. A. Summerville and F. Basolo, *Chem. Rev.*, 1979, **79**, 139.
- 23 M. H. Gubelmann and A. F. Williams, *Struct. Bonding*, 1983, **55**, 1.
- 24 (a) K. Bajdor, K. Nakamoto, H. Kanatomi and I. Murase, *Inorg. Chim. Acta*, 1984, **82**, 207; (b) W. Kanda, H. Okawa, S. Kida, J. Góral and K. Nakamoto, *ibid.*, 1988, **146**, 193.
- 25 K. Nakamoto, *Infrared and Raman Spectra of Inorganic and Coordination Compounds*, Wiley-Interscience, New York, 5th edn., 1997, part B.
- 26 J. M. Burke, J. R. Kincaid, S. Peters, R. R. Gagne, J. P. Collman and T. G. Spiro, *J. Am. Chem. Soc.*, 1978, **100**, 6083.
- 27 F. Inagaki, M. Tasumi and T. Miyazawa, *J. Mol. Spectrosc.*, 1974, **50**, 286.
- 28 M. Gouterman, in *The Porphyrins*, ed. D. Dolphin, Academic Press, New York, 1978, vol. III, part A, ch. 1.
- 29 T. Kitagawa, M. Abe, Y. Kyogoku, H. Ogoshi, E. Watanabe and Z. Yoshida, *J. Phys. Chem.*, 1976, **80**, 1181.
- 30 T. G. Spiro, in *Iron Porphyrins*, ed. A. B. P. Lever and H. B. Gray, Addison-Wesley, Reading (MA), 1983, vol. 2, p. 91.
- 31 X.-Y. Li, Ph.D. Dissertation, Princeton University, 1988.
- 32 N.-T. Yu and E. A. Kerr, in ref. 1, p. 39.
- 33 K. Bajdor, H. Oshio and K. Nakamoto, *J. Am. Chem. Soc.*, 1984, **106**, 7273.
- 34 M. Zerner, M. Gouterman and H. Kobayashi, *Theor. Chim. Acta*, 1966, **6**, 363.
- 35 J. P. Collman, J. L. Hoard, N. Kim, G. Lang and C. A. Reed, *J. Am. Chem. Soc.*, 1975, **97**, 2676.
- 36 K. Bajdor, J. R. Kincaid and K. Nakamoto, *J. Am. Chem. Soc.*, 1984, **106**, 7741.
- 37 K. Nakamoto, I. R. Paeng, T. Kuroi, T. Isobe and H. Oshio, *J. Mol. Struct.*, 1988, **189**, 293.
- 38 L. M. Proniewicz and H. Majcherczyk, *Univ. Jagell. Acta Chim.*, 1993, **36**, 115.
- 39 J. P. Collman, J. I. Brauman, T. R. Halbert and K. S. Suslick, *Proc. Natl. Acad. Sci. USA*, 1976, **73**, 3333.
- 40 C. H. Barlow, J. C. Maxwell, W. J. Wallace and W. S. Caughey, *Biochem. Biophys. Res. Commun.*, 1973, **55**, 91.
- 41 H. Brunner, *Naturwissenschaften*, 1974, **61**, 129.
- 42 J. C. Maxwell, J. A. Volpe, C. H. Barlow and W. S. Caughey, *Biochem. Biophys. Res. Commun.*, 1974, **58**, 166.
- 43 M. Tsubaki, K. Nagai and T. Kitagawa, *Biochemistry*, 1980, **19**, 379.
- 44 J. R. Kincaid, L. M. Proniewicz, K. Bajdor, A. Bruha and K. Nakamoto, *J. Am. Chem. Soc.*, 1985, **107**, 6775.
- 45 W. T. Potter, M. P. Tucker, R. A. Houtchens and W. S. Caughey, *Biochemistry*, 1987, **26**, 4699.
- 46 L. M. Proniewicz and J. R. Kincaid, *Coord. Chem. Rev.*, 1997, **161**, 81.
- 47 L. M. Miller and M. R. Chance, *J. Am. Chem. Soc.*, 1994, **116**, 9662.

Paper 8/05124K